

Active matter invasion of a viscous fluid and a no-flow theorem

Christopher J. Miles*

Department of Physics, University of Michigan, 450 Church St., Ann Arbor, MI 48109, USA

Arthur A. Evans

Department of Mathematics, University of Wisconsin-Madison, 480 Lincoln Dr., Madison, WI 53706, USA

Michael J. Shelley

Flatiron Institute, Simons Foundation, New York, NY, USA; and Courant Institute of Mathematical Sciences, New York University, New York, NY 10012, USA

Saverio E. Spagnolie[†]

Department of Mathematics, University of Wisconsin-Madison, 480 Lincoln Dr., Madison, WI 53706, USA

(Dated: September 1, 2022)

We investigate the dynamics of hydrodynamically interacting motile and non-motile stress-generating swimmers or particles as they invade a surrounding viscous fluid. Colonies of aligned pusher particles are shown to elongate in the direction of particle orientation and undergo a cascade of transverse concentration instabilities. Colonies of aligned puller particles instead are found to elongate in the direction opposite the particle orientation and exhibit dramatic splay as the group moves into the bulk. A linear stability analysis of concentrated line distributions of particles is performed and growth rates are found, using an active slender-body approximation, to match the results of numerical simulations. Thin concentrated bands of aligned pusher particles are always unstable, while bands of aligned puller particles can either be stable (immotile particles) or unstable (motile particles) with a growth rate which is non-monotonic in the force dipole strength. We also prove a surprising “no-flow theorem”: a distribution initially isotropic in orientation loses isotropy immediately but in such a way that results in no fluid flow anywhere and for all time.

The last decade has seen an explosion of interest in the collective dynamics of active particles immersed in fluids, from swimming microorganisms to magnetically driven and phoretic colloidal particles [1–13]. Suspensions of swimming *B. subtilis*, *E. Coli*, and *Myxococcus* cells exhibit such rich behavior as local particle alignment and large-scale organization on length scales much longer than individual particle size [8], enhanced diffusion of tracer particles and mixing flows [14–25], density shock waves [26, 27], energy-independent correlation-lengths [28, 29], and reduced or even negative viscosities [30–39]. Similar features have also been observed in suspensions of spermatozoa [40–43]. There are important biological and human health consequences of this collective organization, including improved bacterial resistance to antibiotic and other threatening agents [44, 45].

Similar features have been observed in suspensions of biofilaments transported through the activity of molecular motors, which also exert hydrodynamic stresses on the surrounding environment. Experiments on kinesin-driven microtubule assemblies have been dynamically rich and have become a model experimental system through which to understand much more complicated biological phenomena such as cell division [46–51].

A popular model of active suspensions is a mean-field kinetic theory which tracks the distribution of particle positions and orientations and which may include hydrodynamic interactions [7, 10, 15, 52, 53] and other short-range physics [53, 54]. Swimmers are classified as either “pushers” or “pullers” depending on the sign of the generated stresslet flow, which in turn depends on the geometry of the swimmer and

the propulsion mechanism [15, 55–59]. Others have modeled these systems as active nematic liquid crystals [60–65] in which, after approximation, the moments of the particle distribution function are evolved directly. Generic features in these systems include long-range coherence, topological defects, and instability [15, 65–70].

Much is known about active suspensions which cover the entire available physical domain. Far less is known about the invasion of a surrounding particle-free environment, though this is of considerable importance in the dynamic self-assembly of swarming organisms [71–73] and in the formation of biofilms, mycelia, and fruiting bodies [74]. Recent explorations on this topic include a rapid expansion of acoustically-trapped swimmers into a bulk fluid [75], a one-dimensional clustering instability [76, 77], and the dynamics of bounded regions of active particles using a Cahn-Hilliard model [78, 79].

In this Letter we investigate numerically and analytically the dynamics of colonies (a coherent collective) of either motile or non-motile active particles as they invade a surrounding viscous fluid. Colonies of aligned pushers are shown to elongate in the direction of particle orientation followed by a cascade of transverse concentration instabilities. Perturbations of an approximate line-distribution of nearly aligned pusher or puller particles result in growth or decay rate which depends on the intensity of active stress, the particle swimming speed, and the mean number density. These rates are understood through an “active slender-body” theory which provides analytical approximations that compare closely with the results of full numerical simulations. We close with a proof

and demonstration of a counter-intuitive *no-flow theorem*, that an isotropically oriented distribution with any initial concentration profile results in no fluid flow everywhere and for all time.

Mathematical model: Following Refs. [15, 53], we describe a suspension of N self-propelled rod-like particles in a viscous fluid by the particle distribution function $\Psi(\mathbf{x}, \mathbf{p}, t)$, where \mathbf{x} is the particle position in a periodic box Ω of length L while \mathbf{p} is the particle orientation vector on a unit sphere S ($|\mathbf{p}| = 1$). The number of swimmers is conserved, $N = \int_{\Omega} \int_S \Psi(\mathbf{x}, \mathbf{p}, t) d\mathbf{p} d\mathbf{x}$, which leads (requiring $dN/dt = 0$) to a Smoluchowski equation,

$$\Psi_t + \nabla \cdot (\dot{\mathbf{x}}\Psi) + \nabla_{\mathbf{p}} \cdot (\dot{\mathbf{p}}\Psi) = 0, \quad (1)$$

where $\nabla = \nabla_{\mathbf{x}}$ and $\nabla_{\mathbf{p}} = (\mathbf{I} - \mathbf{p}\mathbf{p}) \cdot \partial/\partial\mathbf{p}$. The fluxes $\dot{\mathbf{x}}$ and $\dot{\mathbf{p}}$ are given by $\dot{\mathbf{x}} = V_0\mathbf{p} + \mathbf{u}(\mathbf{x}) - d_t\nabla(\ln\Psi)$, and $\dot{\mathbf{p}} = (\mathbf{I} - \mathbf{p}\mathbf{p}) \cdot (\mathbf{p} \cdot \nabla\mathbf{u}) - d_r\nabla_{\mathbf{p}}(\ln\Psi)$, where d_t (d_r) is the translational (rotational) diffusivity, V_0 is the swimming speed, $\mathbf{u}(\mathbf{x}, t)$ is the fluid velocity, and $\mathbf{p}\mathbf{p}$ is a dyadic product.

The environment is assumed to be a viscous Newtonian fluid which moves under an active stress generated by the suspended particles. The flow field \mathbf{u} satisfies the Stokes equations, consisting of momentum balance $-\nabla q + \mu\nabla^2\mathbf{u} + \mathbf{f}_a = \mathbf{0}$ with q the pressure, μ the dynamic viscosity, and $\mathbf{f}_a = \nabla \cdot \Sigma_a$ the active force density, and mass conservation $\nabla \cdot \mathbf{u} = 0$. The active stress Σ_a is given by the mean-field approximation [10]:

$$\Sigma_a(\mathbf{x}) = \sigma\langle\mathbf{p}\mathbf{p}\rangle = \sigma \int_{\Omega} \mathbf{p}\mathbf{p}\Psi(\mathbf{x}, \mathbf{p}, t) d\mathbf{p}, \quad (2)$$

where $\langle\mathbf{p}\mathbf{p}\rangle$ is the second orientational moment of Ψ , and where $\sigma < 0$ for pushers (e.g. *E. coli*) $\sigma > 0$ for pullers. The coefficient σ has been computed for ellipsoidal ‘‘Janus’’ particles [56, 58] and for more general particle types [59], and has been obtained experimentally for a few types of swimming cells [80, 81]. Other orientational moments will appear throughout, and we define $\langle h(\mathbf{p}) \rangle = \int_{\Omega} h(\mathbf{p})\Psi d\mathbf{p}$.

With ℓ the active particle length, we scale velocities by the swimming speed, V_0 , and lengths by the mean-free path $\ell_c = (V/V_p)\ell$, where V is the total fluid volume and $V_p = N\ell^3$ is an effective volume of swimmers, hence $\ell_c = V(N\ell^2)^{-1}$. Time is scaled by ℓ_c/V_0 , force densities are scaled by $\mu V_0/\ell_c^2$, and the particle number density is defined by $n = N/V = (\ell^2\ell_c)^{-1} = (\ell/\ell_c)\ell^{-3}$. Particle conservation is then written as $\kappa^{-1} \int_V \int_S \Psi d\mathbf{p} d\mathbf{x} = 1$, where $\kappa^{-1} = \ell_c^3/V$ is proportional to the particle volume fraction.

With all quantities now assumed dimensionless, the far-field velocity due to an individual swimmer at the origin, oriented in the direction \mathbf{p} , is $\mathbf{u} = \alpha(8\pi)^{-1}\mathbf{p}\mathbf{p} : \nabla\mathbf{G}(\mathbf{x})$, where $\alpha = \sigma/[\mu V_0\ell_c^2]$ is the dimensionless force dipole strength, and $G_{ij} = \delta_{ij}/|\mathbf{x}| + x_i x_j/|\mathbf{x}|^3$ is the Stokeslet singularity [82]. The active force density is then given by $\mathbf{f}_a = \nabla \cdot \Sigma_a = \alpha(\ell_c/\ell)^2 \nabla \cdot \langle\mathbf{p}\mathbf{p}\rangle$. Experiments by Drescher et al. [80, 81] determined that the velocity field far from the body was well approximated as a force dipole with strength $\sigma/(8\pi\mu) = -31.8\mu\text{m}^3/\text{s}$ (see

Fig. 1). Using a cell body size $\ell \approx 3\mu\text{m}$ and swimming speed $V_0 \approx 22\mu\text{m}/\text{s}$, the dimensionless dipole strength for suspensions of *E. coli* are therefore $\alpha \approx -4(\ell/\ell_c)^2$. Following Ref. [15] for the sake of comparison, we set $\ell_c/\ell = 1$ and $\kappa = L_x L_y = 50^2$.

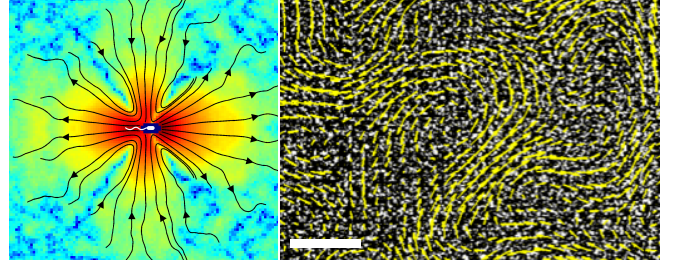


FIG. 1. Left: Experimental particle-image-velocity (PIV) near an *E. coli* cell ([81], with permission). Right: A swimming suspension of *B. subtilis* cells ([29], with permission), overlaid with a PIV flow field. The scale bar is $35\mu\text{m}$; the longest arrows correspond to a velocity of $30\mu\text{m}/\text{s}$.

The dependence of the system on the swimming speed now appears only in the dimensionless dipole strength α ; V_0 is replaced by unity in the particle flux expression for motile systems. In the case of non-motile particles a different velocity scale is required for nondimensionalization [83].

We will assume that particles all move in a direction parallel to the xy -plane, and invariance in the direction perpendicular to it, writing $\Psi(\mathbf{x}, \mathbf{p}, t) = \Psi(x, y, \theta, t)$ and $\mathbf{p} = \cos\theta\hat{\mathbf{x}} + \sin\theta\hat{\mathbf{y}}$. Numerical simulations are carried out in a periodic domain $(x, y, \theta) \in [-L_x/2, L_x/2] \times [-L_y/2, L_y/2] \times [-\pi, \pi)$, using a pseudospectral method with 256^3 gridpoints and dealiasing (zero padding, 3/2 rule) [84]; time-stepping is performed using an integrating factor method along with a second-order accurate Adams-Bashforth scheme.

Self-stretching of an aligned particle colony: We first consider a circular Gaussian colony of nearly aligned particles,

$$\Psi(\mathbf{x}, \theta, t = 0) = C e^{-r^2/a^2 - \theta^2/\varepsilon^2}, \quad (3)$$

where $r = \sqrt{x^2 + y^2}$, C is a numerically-determined normalization constant, and the domain size is large enough to make negligible any effects from periodic spatial boundary conditions. For motile pusher particles with Gaussian radius $a = 4$, angular spread $\varepsilon = 0.2$, and dipole strength $\alpha = -0.5$, numerical simulations reveal a nearly fore-aft symmetric self-stretching in the direction of motion. Perturbing the initial data slightly by setting $r = \sqrt{x^2 + (y - 0.1 \sin(2\pi x/L_x))^2}$ in (3), the dynamics are roughly unchanged for small times, but after the colony becomes sufficiently thin it undergoes a transverse concentration instability, shown in Fig. 2a. Fore-aft symmetry is broken partly by the initial angular spread but primarily due to particle motility; the colony splays at the leading tip on the right, while undergoing a periodic folding at the rear reminiscent of the buckling of planar viscous jets [85] and sedimenting elastic filaments [86].

A puller colony ($\alpha = 0.5$) instead elongates perpendicular

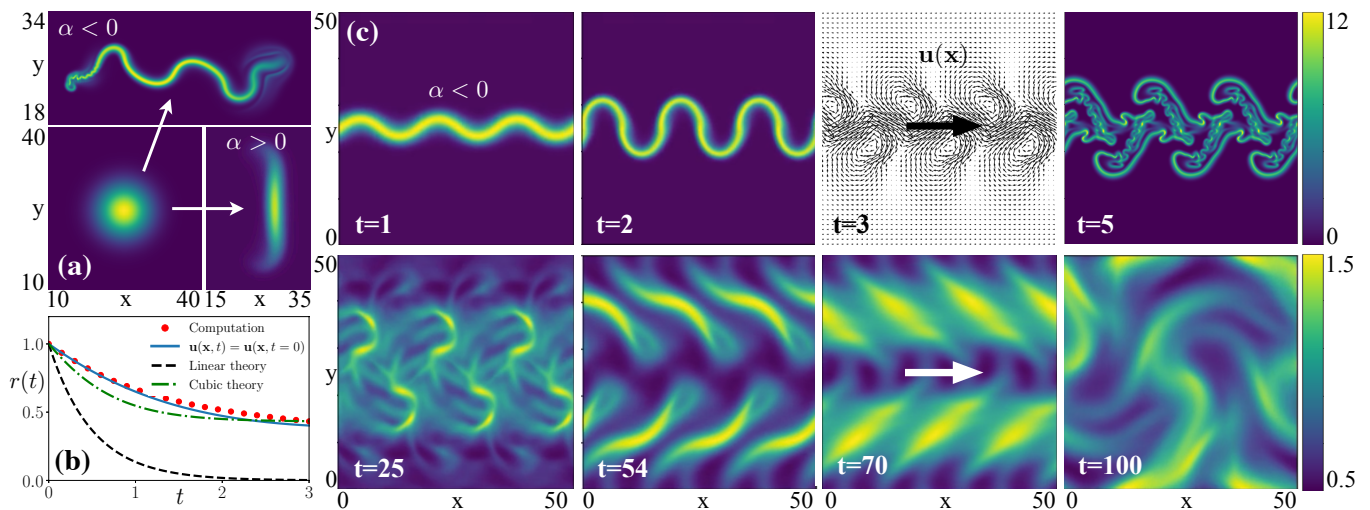


FIG. 2. (a) Evolution of a weakly perturbed Gaussian colony of aligned motile pushers ($\alpha = -0.5$, above) and pullers ($\alpha = 0.5$, right), with concentrations shown at $t = 2.5$. See Supplementary Movie M1. (b) The colony aspect ratio from simulations and different theoretical approximations. (c) Evolution of a thin band of motile pusher particles, $\alpha = -1$, with initial distribution function $\Psi(\mathbf{x}, \theta, t = 0) = C \exp\{-(y - \varepsilon h(x))^2/a^2 - \theta^2/b^2\}$ with C a normalization constant. The initial perturbation is given by $\varepsilon h(x) = 0.1 \sin(6\pi x/L_x)$ and $(a, b) = (2, 0.2)$. Exponential growth in amplitude leads to the development of an internal thrust-wake ($t = 3$) and a buckling cascade to smaller and smaller wavelengths ($t \in [3, 6]$). After passing through numerous almost stationary states, including looped ($t = 54$) and rotating aster ($t = 70$) patterns, symmetry is eventually broken and the suspension arrives in an aperiodic roiling state ($t = 100$). See Supplementary Movie M2.

to the swimming direction (also shown in Fig. 2a), the perturbation appearing never to play a role, and a colony-scale splaying develops on the time-scale associated with the individual swimming speed. Videos of expanding pusher and puller colonies are included as Supplementary Movie M1.

To rationalize the initial self-stretching we consider the dynamics of the moments of Ψ . The concentration of particles, $c = \langle 1 \rangle$, evolves (integrating (1) over θ) via

$$c_t + \nabla \cdot [(\mathbf{u} + V_0^* \mathbf{n})c] = d_t \nabla^2 c, \quad (4)$$

where V_0^* is either 1 or 0 (for motile or non-motile particles, respectively) and $\mathbf{n} = \langle \mathbf{p} \rangle / c$. For short times the velocity field is that due to the initial Gaussian colony. Inserting (3) (for vanishing ε) into (2), and the active stress into the Stokes equations, the velocity field far from the colony takes on the same dipolar form (scaled by κ) as that due to an individual stress-generating particle, $\mathbf{u}(\mathbf{x}) = -\alpha\kappa(x^2 - y^2)\mathbf{x}/[4\pi\mu|\mathbf{x}|^4] + O(|\mathbf{x}|^{-2})$. More pertinent to the self-stretching is the near-field velocity, which (for $|\mathbf{x}| \ll a$) is $\mathbf{u}(\mathbf{x}) = \alpha\kappa(-x, y)/[8\pi\mu a^2] + O(|\mathbf{x}|^2/a^2)$ [83]. There is an immediate connection between the flow due to a Gaussian colony and the flow due to a “regularized Stokeslet” [83, 87].

Figure 2b shows the steadily decreasing aspect ratio $r(t) = b(t)/a(t)$ of a colony of aligned pushers with $\alpha = -1$, with Gaussian initial concentration width $a_0 = 10$. The semi-major axis lengths are defined by $(a(t)^2, b(t)^2) = 2\kappa^{-1} \int_{\mathbb{R}^2} ((x - x_c)^2, (y - y_c)^2) c(\mathbf{x}, t) d\mathbf{x}$, with $\mathbf{x}_c = \kappa^{-1} \int_{\mathbb{R}^2} \mathbf{x} c(\mathbf{x}, t) d\mathbf{x}$. The evolution is captured very well by studying Eq. (4), fixing $\mathbf{n} = \hat{\mathbf{x}}$, and using the velocity field found numerically at $t = 0$, $\mathbf{u}(\mathbf{x}, t) = \mathbf{u}(\mathbf{x}, t = 0)$ (solid line in Fig. 2b). Analyt-

ical predictions follow from Eq. (4) with $\mathbf{n} = \hat{\mathbf{x}}$, and Taylor expanding the velocity field about the center of mass [83]. Using the (fixed at $t = 0$) linear velocity field in the previous paragraph we estimate $r(t) = \exp[\alpha\kappa t/(4\pi a_0^2)]$ (dashed line in Fig. 2b) suggesting a time scale for appreciable changes in shape $\tau \approx 4\pi a_0^2/(|\alpha|\kappa)$. A cubic approximation to the velocity field results in a more accurate prediction, also included in Fig. 2b [83].

Instability of a thin band of pushers: Motivated by the instability observed in the previous section we examine the behavior of an infinitely long distribution of particles which are initially in near alignment. Figure 2c shows the evolution of a distribution of pusher particles with $\alpha = -1$, initially confined to a thin band and with a small transverse perturbation. Early stages show rapid growth of the wave amplitude. At the same time the vorticity field rotates individual particles so that they remain nearly tangent to the concentration band (illustrated in Fig. 3, see Supplementary Movie M2), which results in the same instability playing out again and again on smaller length scales in a cascade reminiscent of a Kelvin-Helmholtz instability. What follows is a transient passage from one seemingly stationary attracting state to another until the system is finally drawn to the aperiodic roiling state described by Saintillan & Shelley [15]. The dynamics suggest the presence of numerous unstable stationary or periodic solutions.

To analyze the instability, let $\varepsilon h(x, t)$ represent the vertical displacement of the line distribution and $\varepsilon \phi(x, t)$ be the mean particle orientation angle ($\cos(\varepsilon \phi) = \hat{\mathbf{x}} \cdot \mathbf{n}$). We study the dynamics of this line distribution through its far-field self-influence. Up to order ε , the active line density of particles is

governed by

$$h_t + V_0^* h_x = v^{(1)}(x, 0, t) + V_0^* \phi, \quad \phi_t + V_0^* \phi_x = v_x^{(1)}(x, 0, t), \quad (5)$$

where $v = \hat{\mathbf{y}} \cdot \mathbf{u} = \varepsilon v^{(1)} \hat{\mathbf{y}}$, and both v and v_x are evaluated on the flat surface where $\varepsilon h(x, t) = 0$ [83]. To close the system we require the self-generated flow. Inserting a line distribution of particles into the active stress integral and carrying this through to the velocity field results in a nonlocal integration over of a line distribution of stresslets, which for $\varepsilon \ll 1$ is given by

$$\mathbf{u}(x) = \frac{-\varepsilon \alpha \kappa}{4\pi L_x} \int_0^{L_x} \frac{h(x, t) - h(x', t)}{(x - x')^2} \hat{\mathbf{y}} dx' + O(\varepsilon^2), \quad (6)$$

to be interpreted in the principal value sense [83]. Assuming periodicity in x and expanding in a spatial Fourier basis, $h(x, t) = \sum_k \hat{h}_k(t) \exp(2\pi i k x / L_x)$, we find

$$\mathbf{u}(x, t) = \frac{-\pi \varepsilon \alpha \kappa}{2L_x^2} \sum_k |k| \hat{h}_k(t) \exp(2\pi i k x / L_x) \hat{\mathbf{y}}. \quad (7)$$

Expressing ϕ similarly, the dynamics are governed at first order in ε by

$$\hat{h}'_k + \frac{2\pi i k V_0^*}{L_x} \hat{h}_k = \frac{-\pi \alpha \kappa |k|}{2\mu L_x^2} \hat{h}_k + V_0^* \hat{\phi}_k, \quad (8)$$

$$\hat{\phi}'_k + \frac{2\pi i k V_0^*}{L_x} \hat{\phi}_k = \frac{-\pi^2 i k |k| \alpha \kappa}{\mu L_x^3} \hat{h}_k, \quad (9)$$

a linear system with eigenvalues

$$\lambda_{\pm} = \frac{\pi}{4L_x^4} \left(-\alpha \kappa |k| - 8i k L_x V_0^* \pm \gamma_k \right), \quad (10)$$

where $\gamma_k = \sqrt{\alpha \kappa (\alpha \kappa k^2 - 16i L_x V_0^* k |k|)}$. A comparison to numerics is shown in Fig. 3 for three negative dipole strengths (pushers) along with the theoretical prediction for a wider range of α and k . The analytical predictions are accurate for

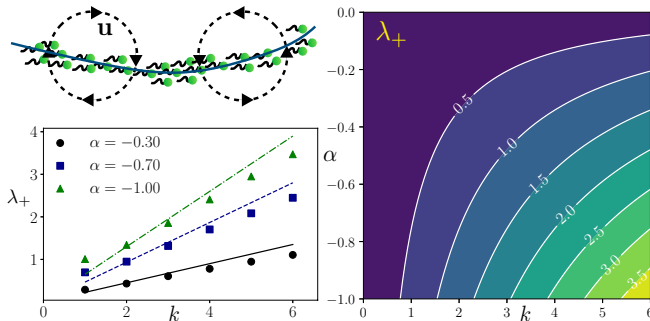


FIG. 3. A thin band of aligned pushers is unstable to transverse concentration perturbations due to its self-generated velocity field. Bottom left: the positive growth rate for motile pushers, comparing numerics and theory. Right: theoretical growth rates for motile pushers for a range of dipole strengths and wave numbers.

the entire range studied, with discrepancies owing to the vertical periodic boundary condition and the non-vanishing thickness of the line distribution in the simulations.

In the non-motile case, $V_0^* = 0$ (or in the limit as $|\alpha|/V_0^* \rightarrow \infty$) line distributions of pushers are all unstable and distributions of pullers are all stable, with respective growth and decay rates both given by $-\pi \alpha \kappa |k| / (2L_x^2)$. This behavior owes to the vorticity field created by the active stress, illustrated in Fig. 3 (see Supplementary Movie M2), which either amplifies or damps the initial concentration perturbation.

In the motile case, $V_0^* = 1$, pusher distributions remain unstable for any $\alpha < 0$. A distribution of pullers, however, excites a very small positive-real-part eigenvalue in (10). Unlike in the case of pushers the maximal eigenvalue is not monotonic in the force dipole strength. Taylor expanding about small α , the largest eigenvalue has approximate value $\alpha = 2L_x/\kappa$, at which point $\text{Re}[\lambda_+] = \pi k (2L_x)^{-1}$ (since $\text{Re}[\lambda_+] \sim \pi \kappa \alpha k (4L_x^2)^{-1}$). The vorticity field (oppositely signed to that illustrated in Fig. 3) rapidly damps the initial displacement, $\varepsilon h(x, t)$, as in the non-motile case, and as in the non-motile pusher case the vorticity rotates the particles towards a direction perpendicular to the concentration band. Introducing motility, however, gives the displacement and orientation fields the freedom towards synchronization with particles most significantly rotated at the wave crests, leading ultimately to rapid growth of the concentration band amplitude (see Supplementary Movie M3) and a large departure away from the initial profile (see Fig. 4).

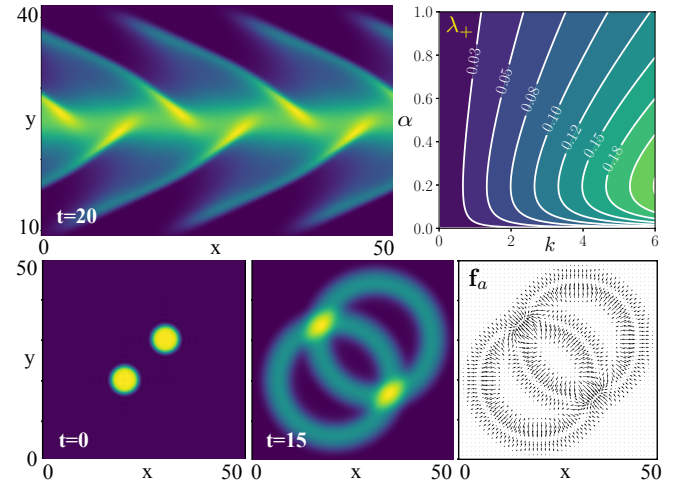


FIG. 4. Top: A thin band of immotile puller particles is stable, but motile particles (shown here with $\alpha = 0.1$ and $d_t = d_r = 0.001$) is unstable. See Supplementary Movie M3. The initial condition is along the unstable eigenvector with wavenumber $k = 3$, $\varepsilon h(x, 0) = 0.144 \cos(6\pi x / L_x) - 0.063 \sin(6\pi x / L_x)$ and $\varepsilon \phi(x, 0) = 0.1 \cos(6\pi x / L_x)$. Growth rates are shown on the right. Bottom: Two circular isotropically oriented colonies expand radially and pass through each other without interacting. The active force $\mathbf{f}_a = \nabla \cdot \Sigma_a$ (right) is curl-free, modifying only the pressure and resulting in no fluid flow, $\mathbf{u} = \mathbf{0}$. This linear superposition generalizes to arbitrary initial concentration fields. See Supplementary Movie M4.

For the motile suspensions above with non-zero dipole strength α there can be competing effects; in particular, if $\max(\text{Re}[\lambda_{\pm}]) < 0$ all solutions to the linear system eventually arrive at the stable base state, but if the system state departs from the linearized region of phase space fast enough such solutions may not be realized in the fully nonlinear dynamics. This potential for departure is seen most clearly if the particles are not stress-generating: with $\alpha = 0$ the wave amplitude grows linearly in time since any particles with nonzero initial orientation angle drift off without resistance along characteristic curves.

Isotropic suspensions remain velocity free: a “no-flow theorem”: Assuming uniqueness of solutions to Eq. (1), active suspensions of motile or immotile particles modeled by Eq. (1) which are initially isotropic in orientation, $\Psi(\mathbf{x}, \mathbf{p}, t = 0) = \Psi_0(\mathbf{x})$, result in no fluid flow, $\mathbf{u}(\mathbf{x}, t) = \mathbf{0}$, everywhere and for all time.

Sketch of the proof: The proof assumes uniqueness of solutions for Eq. (1), which was shown for two-dimensions by Chen & Liu [88]. Consider first the solution Ψ^* to the Smoluchowski equation without velocity terms, $\Psi_t + V_0 \mathbf{p} \cdot \nabla \Psi - d_t \nabla_{\mathbf{x}}^2 \Psi - d_r \nabla_{\mathbf{p}}^2 \Psi = 0$, with an initial condition isotropic in orientation. The velocity field generated by this solution, $\mathbf{u}[\Psi^*]$, is given in Fourier space by $\hat{\mathbf{u}}_{\mathbf{k}}[\Psi^*] = (8\pi|\mathbf{k}|^2)^{-1}(\mathbf{I} - \hat{\mathbf{k}}\hat{\mathbf{k}}) \cdot \hat{\Sigma}_a \cdot \mathbf{k}$, where $\hat{\Sigma}_a \cdot \mathbf{k} = \int_{\Omega} \mathbf{p}(\mathbf{p} \cdot \mathbf{k}) \hat{\Psi}_{\mathbf{k}}^*(\mathbf{p}, t) d\mathbf{p}$ and $\hat{\mathbf{k}} = \mathbf{k}/|\mathbf{k}|$. Writing \mathbf{k} in a spherical (3D) or polar (2D) coordinate system about \mathbf{p} we find $\hat{\Sigma}_a \cdot \mathbf{k} = \lambda_{\mathbf{k}}(t)\mathbf{k}$ for some scalar function $\lambda_{\mathbf{k}}(t)$. Hence $\hat{\mathbf{u}}_{\mathbf{k}}[\Psi^*] = \mathbf{0}$ and then $\mathbf{u}[\Psi^*] = \mathbf{0}$. Since $\mathbf{u}[\Psi^*] = \mathbf{0}$, Ψ^* also solves Eq. (1) with velocity terms included. By uniqueness of solutions to Eq. (1) we finally have that $\mathbf{u} = \mathbf{0}$ everywhere and for all time for any initially isotropic distribution. A more detailed proof is included as Supplementary Material.

The result is surprising since the system immediately loses orientational isotropy (see Supplementary Movie M4), which would suggest the quick onset of a non-trivial flow field. Physically, the active force $\mathbf{f}_a = \nabla \cdot \Sigma_a$ is non-trivial for any $t > 0$ but it is curl-free, so we have by the Helmholtz decomposition theorem that $\mathbf{f}_a = \nabla \chi$ for some scalar field χ , which therefore only acts to modify the pressure in the Stokes equations. As time progresses the force distribution evolves with the local active particle alignment, illustrated for two initially uniform colonies in Fig. 4 (see also Supplementary movie M4). However, due to the no-flow theorem the expanding colony waves simply pass through each other as linear wavefronts. Physics which introduce nonlinearities in Eq. (1), such as near-field steric repulsion, are expected to nullify the result.

Conclusion: We have investigated colonies of active particles emerging into a quiescent fluid. Colony-scale elongation depends on the sign of the active stress and can result in a buckling cascade with growth rates approximately linear in the wavenumber. The stability of line distributions of pullers depend on particle motility with a growth rate which is non-monotonic in the dipole strength. Strikingly, a suspension modeled by pure far-field hydrodynamic interactions which is initially isotropic in orientation, even though isotropy is not preserved, results in no fluid flow. However, a local perturba-

tion to the initial isotropy results in self-straining, elongation, and generation of a global velocity field, just as shown for invasion of a quiescent fluid.

Acknowledgements: This project was initiated at the Woods Hole Oceanographic Institute as part of the Geophysical Fluid Dynamics summer program. Financial support from NSF/NIH (DMS/NIGMS 1661900) and NSF-MRSEC (DMR 767-1121288) is gratefully acknowledged.

* cmiless@umich.edu

† spagnolie@math.wisc.edu

- [1] T. J. Pedley and J. O. Kessler, *Annu. Rev. Fluid Mech.* **24**, 313 (1992).
- [2] C. Dombrowski, L. Cisneros, S. Chatkaew, R. E. Goldstein, and J. O. Kessler, *Phys. Rev. Lett.* **93**, 098103 (2004).
- [3] L. H. Cisneros, R. Cortez, C. Dombrowski, R. E. Goldstein, and J. O. Kessler, *Exp. Fluids* **43**, 737 (2007).
- [4] P. T. Underhill, J. P. Hernandez-Ortiz, and M. D. Graham, *Phys. Rev. Lett.* **100**, 248101 (2008).
- [5] A. Baskaran and M. M. Cristina, *Proc. Natl. Acad. Sci USA* **106**, 15567 (2009).
- [6] S. Ramaswamy, *Annu. Rev. Condens. Matter Phys.* **1**, 323 (2010).
- [7] D. L. Koch and G. Subramanian, *Annu. Rev. Fluid Mech.* **43**, 637 (2011).
- [8] T. Vicsek and A. Zafeiris, *Phys. Rep.* **517**, 71 (2012).
- [9] M. C. Marchetti, J. F. Joanny, S. Ramaswamy, T. B. Liverpool, J. Prost, M. Rao, and R. A. Simha, *Rev. Mod. Phys.* **85**, 1143 (2013).
- [10] D. Saintillan and M. J. Shelley, in *Complex Fluids in Biological Systems* (Springer, 2015), pp. 319–351.
- [11] J. Elgeti, R. G. Winkler, and G. Gompper, *Rep. Prog. Phys.* **78**, 056601 (2015).
- [12] A. Zöttl and H. Stark, *J. Phys. Cond. Matt.* **28**, 253001 (2016).
- [13] K. Yeo, E. Lushi, and P. M. Vlahovska, *Soft Matter* **12**, 5645 (2016).
- [14] M. J. Kim and K. S. Breuer, *Anal. Chem.* **79**, 955 (2007).
- [15] D. Saintillan and M. J. Shelley, *Phys. Fluids* **20**, 123304 (2008).
- [16] C. W. Wolgemuth, *Biophys. J.* **95**, 1564 (2008).
- [17] K. C. Leptos, J. S. Guasto, J. P. Gollub, A. I. Pesci, and R. E. Goldstein, *Phys. Rev. Lett.* **103**, 198103 (2009).
- [18] A. Sokolov, R. E. Goldstein, F. I. Feldchtein, and I. S. Aranson, *Phys. Rev. E* **80**, 031903 (2009).
- [19] X.-L. Wu and A. Libchaber, *Phys. Rev. Lett.* **84**, 3017 (2000).
- [20] H. Kurtuldu, J. S. Guasto, K. A. Johnson, and J. P. Gollub, *Proc. Natl. Acad. Sci. USA* **108**, 10391 (2011).
- [21] Z. Lin, J.-L. Thiffeault, and S. Childress, *J. Fluid Mech.* **669**, 167 (2011).
- [22] A. Morozov and D. Marenduzzo, *Soft Matter* **10**, 2748 (2014).
- [23] J.-L. Thiffeault, *Phys. Rev. E* **92**, 023023 (2015).
- [24] A. E. Patteson, A. Gopinath, P. K. Purohit, and P. E. Arratia, *Soft Matter* **12**, 2365 (2016).
- [25] P. Mueller and J.-L. Thiffeault, *Phys. Rev. Fluids* **2**, 013103 (2017).
- [26] A. H. Tsang and E. Kanso, *Phys. Rev. Lett.* **116**, 048101 (2016).
- [27] M. Driscoll, B. Delmotte, M. Youssef, S. Sacanna, A. Donev, and P. Chaikin, *Nature Phys.* **13**, 375 (2017).
- [28] A. Sokolov and I. S. Aranson, *Phys. Rev. Lett.* **109**, 248109 (2012).

- [29] J. Dunkel, S. Heidenreich, K. Drescher, H. H. Wensink, M. Bär, and R. E. Goldstein, *Phys. Rev. Lett.* **110**, 228102 (2013).
- [30] Y. Hatwalne, S. Ramaswamy, M. Rao, and R. A. Simha, *Phys. Rev. Lett.* **92**, 118101 (2004).
- [31] B. M. Haines, I. S. Aranson, L. Berlyand, and D. A. Karpee, *Phys. Biol.* **5**, 046003 (2008).
- [32] A. Sokolov and I. S. Aranson, *Phys. Rev. Lett.* **103**, 148101 (2009).
- [33] D. Saintillan, *Phys. Rev. E* **81**, 056307 (2010).
- [34] L. Giomi, T. B. Liverpool, and M. C. Marchetti, *Phys. Rev. E* **81**, 051908 (2010).
- [35] V. Gyrya, K. Lipnikov, I. S. Aranson, and L. Berlyand, *J. Math. Biol.* **62**, 707 (2011).
- [36] J. Gachelin, G. Miño, H. Berthet, A. Lindner, A. Rousselet, and E. Clément, *Phys. Rev. Lett.* **110**, 268103 (2013).
- [37] Y. Bozorgi and P. T. Underhill, *Rheologica Acta* **53**, 899 (2014).
- [38] H. M. López, J. Gachelin, C. Douarache, H. Auradou, and E. Clément, *Phys. Rev. Lett.* **115**, 028301 (2015).
- [39] R. Alonso-Matilla, B. Ezhilan, and D. Saintillan, *Biomicrofluidics* **10**, 043505 (2016).
- [40] I. H. Riedel, K. Kruse, and J. Howard, *Science* **309**, 300 (2005).
- [41] A. Creppy, O. Praud, X. Druart, P. L. Kohnke, and F. Plouraboué, *Phys. Rev. E* **92**, 032722 (2015).
- [42] A. Creppy, F. Plouraboué, O. Praud, X. Druart, S. Cazin, H. Yu, and P. Degond, *J. Roy. Soc. Interface* **13**, 20160575 (2016).
- [43] S. F. Schoeller and E. E. Keaveny, *arXiv preprint arXiv:1801.08180* (2018).
- [44] M. T. Butler, Q. Wang, and R. M. Harshey, *Proc. Natl. Acad. Sci.* **107**, 3776 (2010).
- [45] F. J. H. Hol, B. Hubert, C. Dekker, and J. E. Keymer, *ISME J* **10**, 30 (2016).
- [46] K. J. Helmke, R. Heald, and J. D. Wilbur, *Int. Rev. Cell Mol. Biol.* **306**, 83 (2013).
- [47] T. Sanchez, D. T. N. Chen, S. J. DeCamp, M. Heymann, and Z. Dogic, *Nature* **491**, 431 (2012).
- [48] F. C. Keber, E. Loiseau, T. Sanchez, S. J. DeCamp, L. Giomi, M. J. Bowick, M. C. Marchetti, A. Dogic, and A. R. Bausch, *Science* **345**, 1135 (2014).
- [49] J. Prost, F. Jülicher, and J.-F. Joanny, *Nature Phys.* **11**, 111 (2015).
- [50] M. J. Shelley, *Annu. Rev. Fluid Mech.* **48**, 487 (2016).
- [51] I. Maryshev, D. Marenduzzo, A. B. Goryachev, and A. Morozov, *Phys. Rev. E* **97**, 022412 (2018).
- [52] D. Saintillan and M. J. Shelley, *Phys. Rev. Lett.* **99**, 058102 (2007).
- [53] G. Subramanian and D. L. Koch, *J. Fluid Mech.* **632**, 359 (2009).
- [54] V. Mehandia and P. R. Nott, *J. Fluid Mech.* **595**, 239 (2008).
- [55] E. Lauga and T. Powers, *Rep. Prog. Phys.* **72**, 096601 (2009).
- [56] S. E. Spagnolie and E. Lauga, *J. Fluid Mech.* **700**, 105 (2012).
- [57] S. Ghose and R. Adhikari, *Phys. Rev. Lett.* **112**, 118102 (2014).
- [58] E. Lauga and S. Michelin, *Phys. Rev. Lett.* **117**, 148001 (2016).
- [59] B. Nasouri and G. J. Elfring, *arXiv* (2018).
- [60] S. Ramaswamy, R. A. Simha, and J. Toner, *Euro. Phys. Lett.* **62**, 196 (2003).
- [61] F. G. Woodhouse and R. E. Goldstein, *Phys. Rev. Lett.* **109**, 168105 (2012).
- [62] M. G. Forest, Q. Wang, and R. Zhou, *Soft Matter* **9**, 5207 (2013).
- [63] L. Giomi, M. J. Bowick, X. Ma, and M. C. Marchetti, *Phys. Rev. Lett.* **110**, 228101 (2013).
- [64] S. P. Thampi, R. Golestanian, and J. M. Yeomans, *Phys. Rev. Lett.* **111**, 118101 (2013).
- [65] T. Brotto, J.-B. Caussin, E. Lauga, and D. Bartolo, *Phys. Rev. Lett.* **110**, 038101 (2013).
- [66] R. A. Simha and S. Ramaswamy, *Phys. Rev. Lett.* **89**, 058101 (2002).
- [67] C. Hohenegger and M. J. Shelley, *Phys. Rev. E* **81**, 046311 (2010).
- [68] E. Bertin, H. Chaté, F. Ginelli, S. Mishra, A. Peshkov, and S. Ramaswamy, *New J. Phys.* **15**, 085032 (2013).
- [69] B. Ezhilan, M. J. Shelley, and D. Saintillan, *Phys. Fluids* **25**, 070607 (2013).
- [70] X. Shi, H. Chaté, and Y. Ma, *New J. Physics* **16**, 035003 (2014).
- [71] J. A. Shapiro, M. Dworkin, et al., *Bacteria as multicellular organisms* (Oxford University Press, 1997).
- [72] M. F. Copeland and D. B. Weibel, *Soft Matter* **5**, 1174 (2009).
- [73] N. C. Darnton, L. Turner, S. Rojevsky, and H. C. Berg, *Biophys. J.* **98**, 2082 (2010).
- [74] D. Claessen, D. E. Rozen, O. P. Kuipers, L. Søggaard-Andersen, and G. P. Van Wezel, *Nature Rev. Microbiol.* **12**, 115 (2014).
- [75] S. C. Takatori, R. De Dier, J. Vermant, and J. F. Brady, *Nature Comm.* **7** (2016).
- [76] L. Jibuti, L. Qi, C. Misbah, W. Zimmermann, S. Rafai, and P. Peyla, *Phys. Rev. E* **90**, 063019 (2014).
- [77] E. Lauga and F. Nadal, *Europhys. Lett.* **116**, 64004 (2017).
- [78] T. Gao and Z. Li, *Physical Review Letters* **119**, 108002 (2017).
- [79] T. Gao, M. D. Betterton, A.-S. Jhang, and M. J. Shelley, *Phys. Rev. Fluids* **2**, 093302 (2017).
- [80] K. Drescher, R. E. Goldstein, N. Michel, M. Polin, and I. Tuval, *Phys. Rev. Lett.* **105**, 168101 (2010).
- [81] K. Drescher, J. Dunkel, L. Cisneros, S. Ganguly, and R. E. Goldstein, *Proc. Natl. Acad. Sci. USA* **108**, 10940 (2011).
- [82] C. Pozrikidis, *Boundary Integral and Singularity Methods for Linearized Viscous Flow* (Cambridge University Press, Cambridge, UK, 1992).
- [83] [], We direct the reader to the supplementary material. [] (2018).
- [84] B. Fornberg, *A practical guide to pseudospectral methods*, vol. 1 (Cambridge university press, 1998).
- [85] J. Cruickshank and B. R. Munson, *J. Fluid Mech.* **113**, 221 (1981).
- [86] L. Li, H. Manikantan, D. Saintillan, and S. E. Spagnolie, *J. Fluid Mech.* **735**, 705 (2013).
- [87] R. Cortez, *SIAM J. Sci. Comput.* **23**, 1204 (2001).
- [88] X. Chen and J.-G. Liu, *J. Differential Equations* **254**, 2764 (2013).